NANO LETTERS

Letter

pubs.acs.org/NanoLett

Three-Dimensional Plasmonic Chiral Tetramers Assembled by DNA Origami

Xibo Shen,[†] Ana Asenjo-Garcia,[‡] Qing Liu,[†] Qiao Jiang,[†] F. Javier García de Abajo,[‡] Na Liu,*[,§] and Baoquan Ding*[,†]

[†]National Center for Nanoscience and Technology, No. 11 BeiYiTiao, ZhongGuanCun, Beijing 100190, China

[‡]IQFR-CSIC, Serrano 119, 28006 Madrid, Spain

[§]Max-Planck-Institute for Intelligent Systems, Heisenbergstrasse 3, D-70569 Stuttgart, Germany

Supporting Information

ABSTRACT: Molecular chemistry offers a unique toolkit to draw inspiration for the design of artificial metamolecules. For a long time, optical circular dichroism has been exclusively the terrain of natural chiral molecules, which exhibit optical activity mainly in the UV spectral range, thus greatly hindering their significance for a broad range of applications. Here we demonstrate that circular dichroism can be generated with artificial plasmonic chiral nanostructures composed of the minimum number of spherical gold nanoparticles required for three-dimensional (3D) chirality. We utilize a rigid addressable DNA origami template to precisely organize four nominally identical gold nanoparticles into a three-dimensional asymmetric tetramer. Because of the chiral structural symmetry and the strong plasmonic resonant coupling between the gold nanoparticles, the 3D plasmonic assemblies undergo different interactions with left and right circularly polarized light, leading to pronounced circular dichroism. Our experimental results agree well with theoretical predictions. The simplicity of our structure geometry and, most importantly, the concept of resorting on biology to produce artificial photonic functionalities open a new pathway to designing smart artificial plasmonic nanostructures for large-scale production of optically active metamaterials.

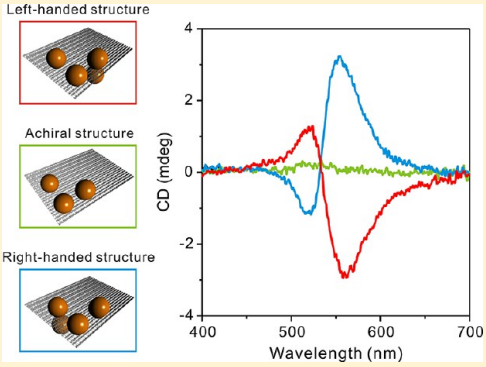

KEYWORDS: *DNA origami, gold nanoparticles, self-assembly, plasmonic, chiral*

Chiral molecules play a pivotal role in biochemistry. Their highly specific interlocking provides an essential motif in the architecture of biomachinery and biochemical cycles.[1] For example, drugs based upon different enantiomers of synthetic chiral chemical compounds can have very different pharmacological effects, mainly because the proteins to which they bind are also chiral. Chemical discrimination of enantiomers can be only carried out in an asymmetric environment, for example by examining how they affect polarized light. Specifically, chiral molecules can absorb different amounts of left and right circularly polarized light, a property that is known as circular dichroism (CD).

Natural chiral molecules such as amino acids, peptides, DNA, and so forth only exhibit CD response in the UV range. Very recently, optical chirality has branched out into the visible and infrared ranges thanks to the introduction of artificial plasmonic structures.[2,3] Both top-down[4−9] and bottom-up[10,11] approaches have been directed toward realizing 3D plasmonic chiral structures exhibiting strong optical chirality. The 3D chiral structures, including gold spirals or twisted gammadions and split-ring resonators that closely resemble the configuration of DNA helices, have been demonstrated using direct laser writing[4] or electron-beam lithography[5,7] techniques. Nevertheless, these plasmonic structures, which are extremely costly for mass production of large-scale areas, generally reside on substrates and operate under forward or backward illumination conditions. Over the past few years, the bottom-up approach has gathered momentum, fueled by the efforts of biochemists to rationalize the organization of metallic nanoparticles into 3D architectures. For example, peptide amphiphile supramolecules have been utilized as chiral scaffolds to directly grow gold nanoparticles (AuNPs) through gold nucleation from precursor salt solutions.[12] Also, DNA nanostructures have been used as templates for the construction of helical AuNP chains.[11,13,14]

While molecular chirality encompasses a vast variety of structural characteristics, most chiral molecules are commonly formed when asymmetric centers are present. For instance, in an α-amino acid four different substituents, COOH, R, NH_2, and H, are bonded to a tetravalent carbon atom, which forms a chiral center, also known as a stereogenic center. This tetrahedral molecular architecture gives rise to two enantiomers, which are nonsuperimposable mirror images of each other. Such tetrahedral chiral molecules imprint a "twist" character to their electronic clouds due to interacting chromophores, which can be

Received: February 11, 2013
Revised: March 18, 2013
Published: April 19, 2013

ACS Publications © 2013 American Chemical Society

characterized as single dipoles. The "twist" feature generates handedness within the chiral molecules, resulting in their unique interaction with circularly polarized light.

The chiral tetrahedrons that represent the most fundamental biological entities, α-amino acids, serve as inspiration to design smart artificial plasmonic nanostructures that exhibit unprecedented photonic functionalities. A pioneering attempt to build a plasmonic analogue of a natural chiral molecule was carried out by Mastroianni et al. in 2009.[15] Four different-sized AuNPs monofunctionalized with single strands of DNA were assembled into a tetrahedron through programmable DNA hybridization. Nevertheless, due to the absence of strong plasmonic coupling and the floppiness of single-stranded DNA, CD was not observed in these plasmonic assemblies. Here we utilize an alternative method, structural DNA nanotechnology,[16−20] to assemble four identical AuNPs in an asymmetric tetrahedron. In fact, four is the minimum number of identical spherical nanoparticles that allows obtaining 3D chirality.[21−26] The AuNPs are organized at four designated binding sites on a rigid DNA origami template[27−31] with spatial accuracy on the nanometer scale. We experimentally demonstrate strong CD in both left-handed and right-handed structures. We show that plasmonic resonant coupling is a critical element to achieve strong CD response. The experimental results are in accordance to theoretical predictions. The strategy of organizing plasmonic particles using DNA origami adds great flexibility for developing sophisticated 3D plasmonic nanostructures, which still remain a significant challenge for top-down techniques. In addition, our approach is scalable and can be used for large-scale mass production of strongly chiral media, which can have applications in chiral sensing (i.e., detection and determination of natural chiral molecules) and in the fabrication of plasmonic metamaterials with engineered functionalities.

Figure 1 illustrates the experimental scheme. Rectangle-shaped DNA origami was first formed by annealing the M13 scaffold strand, capture strands, and helper strands in a ratio of 1:5:10 from 90 °C to room temperature. The product was then purified with a filter device [100 kD, molecular weight cutoff (MWCO), Amicon, Millipore] to remove the extra helper and capture stands. The dimensions of the rectangular origami were roughly 90 nm × 60 nm × 2 nm. DNA capture strands (in different colors) with carefully designed sequences were extended from the rectangular DNA template at four specific positions to precisely organize four AuNPs (20 nm) as shown in Figure 1. Three binding sites were defined on the top surface of the DNA template and the fourth site was positioned on the opposite side, directly below one of the three binding sites on the top surface. Left- and right-handed structures were obtained by arranging the four binding sites in left- and right-handed fashions, respectively. At each binding site, four identical-sequence capture strands were used to assemble one single AuNP. To avoid nonspecific binding, the sequences of the capture strands were all different at the four individual binding sites. The purified DNA origami and AuNPs functionalized with corresponding complementary DNA strands were then mixed and annealed from 43 °C to 23 °C for 24 h. After DNA hybridization, the AuNPs were assembled at the desired four binding sites on the DNA template. As a control experiment, we also fabricated an achiral structure, composed of only three AuNPs on one surface of the rectangular DNA origami following similar experimental procedures (see Supporting Information (SI)).

Subsequently, the annealed product was analyzed by agarose gel electrophoresis. The resulting gel image is shown in Figure 2a. Lanes 1 and 2 correspond to the M13 strand and the rectangular

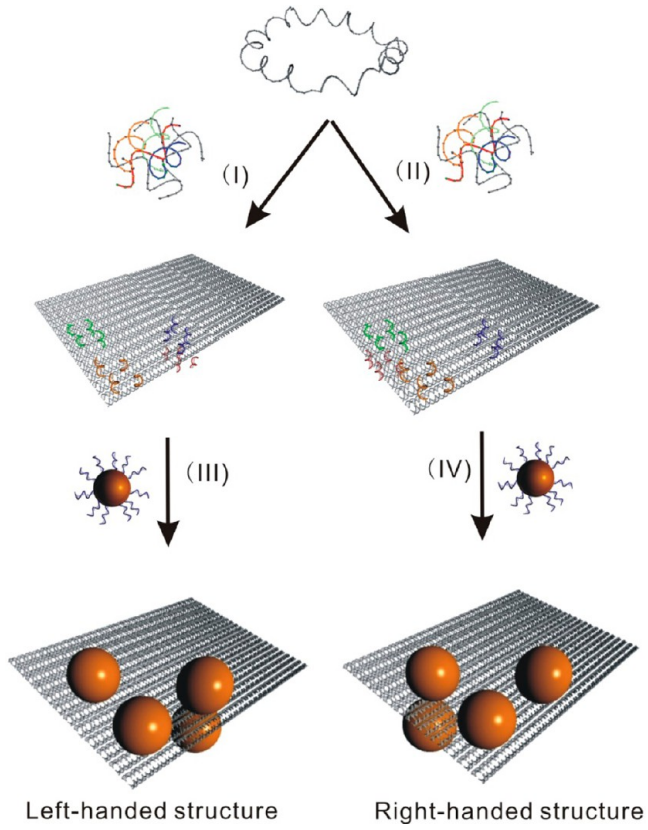

Figure 1. Schematic illustration of the experiment. A long scaffold single DNA strand (M13) hybridizes with helper and capture strands to form a rectangular DNA origami template with well-defined binding sites. The capture strands are extended from four binding sites, three on the top surface and one on the bottom surface of the origami template. These four binding sites are arranged in left- (I) and right-handed (II) configurations for left- and right-handed structures, respectively. Gold nanoparticles (AuNPs, 20 nm) functionalized with corresponding complementary DNA strands are assembled at the predesignated locations on the origami template through DNA hybridization, forming left- (III) and right-handed (IV) structures, respectively.

DNA origami, respectively. Lane 3 corresponds to the thiolated-DNA modified AuNPs. Lanes 4 and 5 contain the left- and right-handed nanostructures, respectively. Lane 6 corresponds to the achiral structures. Bands of the target complexes are highlighted with white-dashed lines. The three target gel bands were then sliced and extracted by electroelution with dialysis tubing membranes (MWCO: 50K). Figure 2b,c shows transmission electron microscopy (TEM) images of left- and right-handed structures, respectively. In order to obtain 3D geometrical information of the structures, stereographic TEM imaging was carried out at different tilting angles. The schematic illustrations in the insets, constructed by taking into account the tilting angle, clearly show the chiral character of the structures. The 0° illustrations in Figure 2b,c are defined to match the TEM images of the left- and right-handed AuNP assemblies before tilting, respectively. The tilting angles are indicated in the TEM images. As shown in Figure 2b,c, the TEM images match the schematic illustrations at different tilting angles very well, demonstrating the 3D characteristics of our chiral assemblies. TEM images of the achiral structures composed of three AuNPs on the DNA origami are provided in SM.

All plamonic structures in this study were dispersed in a TAE/Mg^{2+} buffer (water-based) during optical measurements. Ultra-

dx.doi.org/10.1021/nl400538y | Nano Lett. 2013, 13, 2128−2133

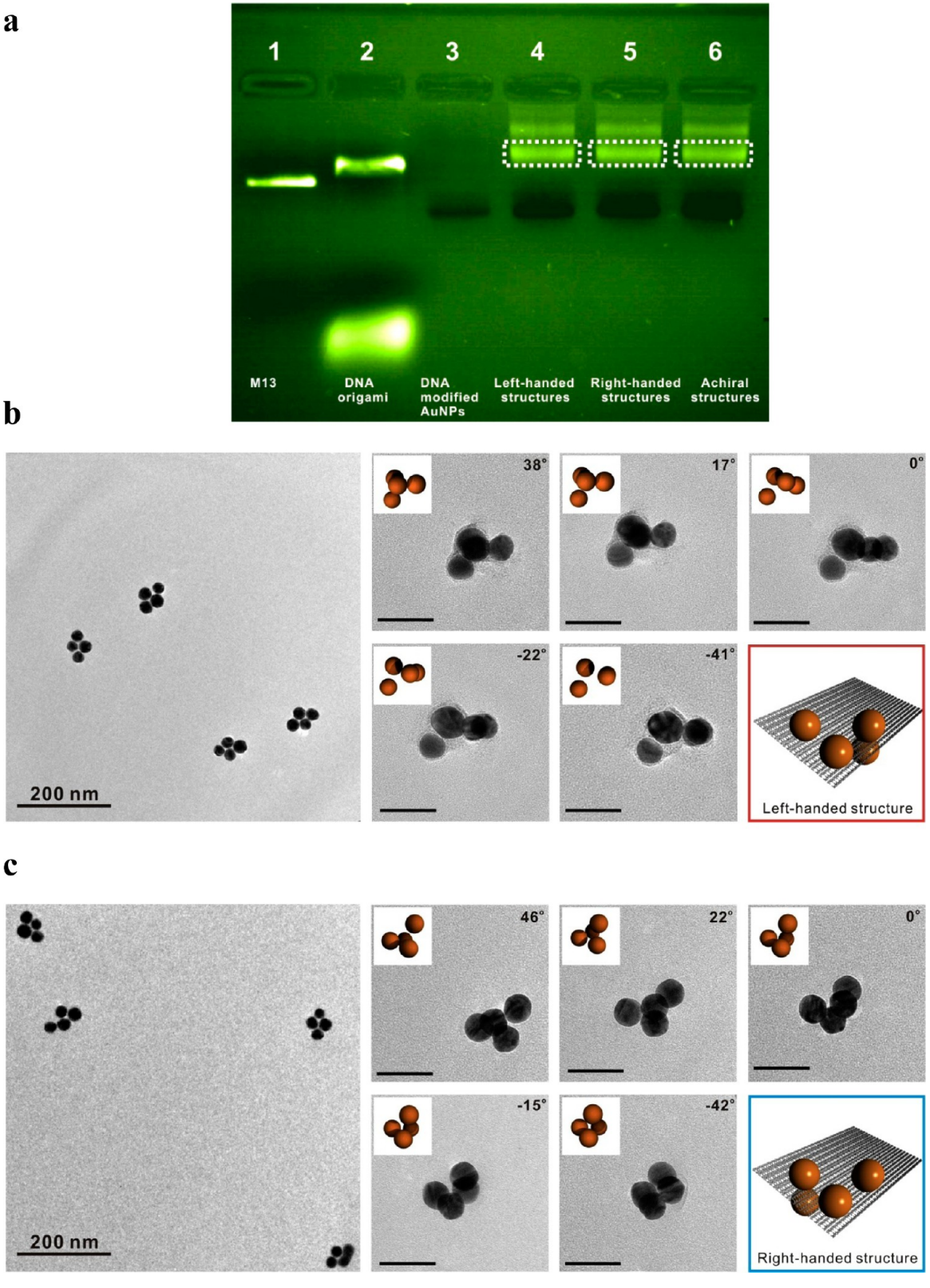

Figure 2. Agarose gel image and TEM images of the left- and right-handed structures. (a) Ethidium bromide-stained agarose gel of the products at different experimental stages. Lane 1: M13. Lane 2: rectangular DNA origami. Lane 3: DNA-modified AuNPs. Lane 4: left-handed structures. Lane 5: right-handed structures. Lane 6: achiral structures. The target products are contained in the bands that are highlighted using white dashed lines. (b) Left: Overview TEM image of several left-handed structures. Right: TEM images of an individual left-handed structure at different titling angles, which are well matched by the schematic illustrations shown as insets. (c) Same as (b) for right-handed structures. The scale bars are 50 nm.

violet−visible (UV−vis) extinction spectra of the left- and right-handed chiral assemblies are shown by red and blue lines in Figure 3a, respectively. The two spectra nearly coincide with each other. For comparison, the UV−vis extinction spectra of the

dx.doi.org/10.1021/nl400538y | *Nano Lett.* 2013, 13, 2128−2133

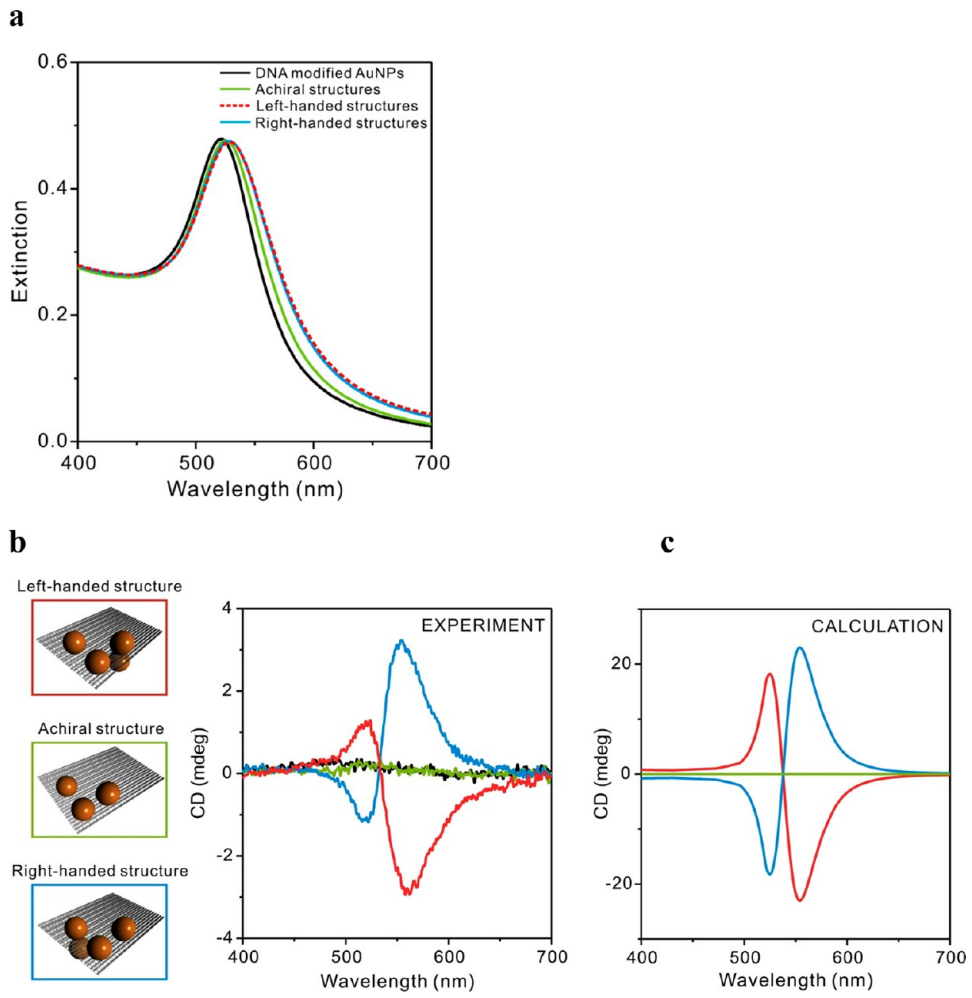

Figure 3. Optical characterization of the DNA assembled structures. (a) UV−vis extinction spectra of the DNA-modified AuNPs (black), achiral (green), left- (red) and right-handed (blue) structures. Measured (b) and calculated (c) CD spectra of these structures, using the same color codes.

DNA modified individual AuNPs (black line) and the achiral assemblies (green line) are also shown in Figure 3a. The spectra of the achiral, left- and right-handed assemblies display clear redshifts compared to that of the DNA modified AuNPs. This is mainly due to the strong near-field coupling between the AuNPs in the assembled structures. Specifically, the spectra of the left- and right-handed structures show a more pronounced redshift than that of the achiral structure, demonstrating the role of the fourth AuNP in the assembly. In order to characterize the chiral response of the 3D AuNP assemblies, CD measurements were carried out with a quartz cuvette (0.5 cm path length) using a J-810 Circular Dichroism Spectrometer. Figure 3b shows the measured CD spectra for left- and right-handed assemblies (red and blue lines, respectively). The left-handed sample presents a characteristic bisignate peak-dip CD shape. The spectrum flips when the handedness is changed, forming a bisignate dip-peak CD profile in the case of the right-handed sample. The bisignate CD line shape indicates the isotropic nature of our samples. This is quite different from the spectral response of the chiral plasmonic tetramers obtained from electron-beam lithography. Those structures preferentially show response to circularly polarized light upon forward or backward illumination conditions, as they stand still along one direction on the substrate.[8] In contrast, our samples contain chiral assemblies that are oriented along all possible directions with respect to the incident circularly polarized light as they can freely move in water. The chiral response of our samples is due to the strong plasmonic resonant coupling between the AuNPs in individual assemblies. More specifically, the 3D arrangement of the four AuNPs in the assembly imprints a "corkscrew" character to the collective plasmons, introducing a twist of specific handedness into the propagation direction of light. It is apparent that the CD spectrum of the achiral sample formed by only three AuNPs does not exhibit CD response, as shown by the green line in Figure 3b. As another control experiment, we measured the CD spectrum of the DNA modified individual AuNPs (Figure 3b, black line), which does not reveal any CD response within the wavelength range of interest. Therefore, the CD response observed in our experiments is due to the plasmonic resonant coupling of the four AuNPs arranged in a 3D chiral geometry.

In order to further understand the underlying physics, we carried out classical electrodynamics calculations taking into account the full multipolar response of the AuNPs via a multiple-scattering formalism[32,33] (see SI). Despite the small size of the AuNPs compared to the light wavelength, the high-order multipoles play an important role to fully describe the collective plasmons of the closely spaced AuNPs (diameter 20 nm, spacing 8 nm). As the orientations of the chiral assemblies in water are totally random, we compute the CD as

$$\mathrm{CD} \propto \langle \sigma_L - \sigma_R \rangle_\Omega \quad (1)$$

dx.doi.org/10.1021/nl400538y | *Nano Lett.* 2013, 13, 2128−2133

where σ_L and σ_R are the extinction cross sections of a chiral tetramer in response to left and right circularly polarized light, respectively, and $\langle\rangle_\Omega$ represents the average over the solid angle of the tetramer orientations. The CD signal is further proportional to both the concentration of the chiral assembly solution and the optical path length (see SI). Figure 3c shows the calculated CD spectra, which are in a qualitatively good agreement with our experimental results. The CD signal amplitudes in the experiment are lower than those in the calculation, mainly because we use in the latter a nominal DNA origami concentration (0.3 nM) as an estimate of the chiral assembly concentration (see SI), which cannot be directly determined from the experiment. The actual concentration is lower, as indicated by the fact that the chiral assemblies were only part of the final products (see the bands in lanes 4 and 5 of Figure 2a). Additionally, the CD response is very sensitive to imperfections of the samples, for example the slight AuNP size and separation variations in the individual assemblies (see SI), which contribute to the lower amplitude and broader profile of the measured CD signal.

Our concept of 3D plasmonic chiral tetramers embodies a successful implementation of molecular models translated from chemistry to nanophotonics. We have employed in our study structural DNA technology to create plasmonic chiral assemblies that are truly 3D isotropic. We have demonstrated that chiral structural symmetry and plasmonic resonant coupling are both essential ingredients for achieving strong optical chirality in artificial plasmonic chiral molecules. These conclusions are supported by theoretical modeling, in excellent agreement with experiment. An important application enabled by our plasmonic chiral tetramers is chiral sensing, wherein the bending or cleavage of specific strands that are used to link the AuNPs on the scaffold can perturb the symmetry of the chiral tetramer. It can cause immediate CD spectral changes, thus providing information that would be otherwise difficult to access via conventional structural determination methods such as macromolecular crystallography or nuclear magnetic resonance spectroscopy. Our approach can also be used to assemble other metal nanoparticles for extending the spectral range of CD response (e.g., silver for higher energies). From a more general perspective, our study further inaugurates a scalable approach toward synthesizing isotropic dispersions of chiral metamolecules of increasing complexity depending on the sequencing of the DNA scaffold and possibly containing nanoparticles of different sizes and compositions selectively assembled at designated locations, thus resulting in artificial optical nanostructures that mimic the complexity of natural biological systems.

■ ASSOCIATED CONTENT

Supporting Information

Details of methods and additional TEM images. This material is available free of charge via the Internet at http://pubs.acs.org.

■ AUTHOR INFORMATION

Corresponding Author

*E-mail: (B.D.) dingbq@nanoctr.cn and (N.L.) laura.liu@is.mpg.de.

Author Contributions

N.L. and B.D. conceived the experiments. X.S., Q.L. and Q.J. performed the experiments. A.A.-G. and F.J.G.d.A. carried out the calculations. N.L., B.D., A.A.-G., and F.J.G.d.A. analyzed the data and wrote the manuscript.

Notes

The authors declare no competing financial interest.

■ ACKNOWLEDGMENTS

B.D. was supported by National Basic Research Program of China (973 Program, 2012CB934000), 100-Talent Program of Chinese Academy of Sciences, National Science Foundation China (21173059, 91127021, 21222311) and Beijing Natural Science Foundation (2122057). N.L. was supported by the Sofja Kovalevskaja Award from the Alexander von Humboldt-Foundation. F.J.G.d.A. acknowledges support from the Spanish MEC (MAT2010-14885 and Consolider NanoLight.es). A.A.-G. acknowledges financial support through FPU from the Spanish ME.

■ REFERENCES

(1) Berova, N.; Nakanishi, K.; Woody, R. W. *Circular Dichroism: Principles and Applications*, VCH: New York, 1994.
(2) Noguez, C.; Garzon, I. L. *Chem. Soc. Rev.* **2009**, *38*, 757.
(3) Xia, Y. H.; Zhou, Y. L.; Tang, Z. Y. *Nanoscale* **2011**, *3*, 1374.
(4) Gansel, J. K.; Thiel, M.; Rill, M. S.; Decker, M.; Bade, K.; Saile, V.; von Freymann, G.; Linden, S.; Wegener, M. *Science* **2009**, *325*, 1513.
(5) Rogacheva, A. V.; Fedotov, V. A.; Schwanecke, A. S.; Zheludev, N. I. *Phys. Rev. Lett.* **2006**, *97*, 177401.
(6) Wegener, M.; Zheludev, N. I. *J. Opt. A: Pure Appl. Opt.* **2009**, *11*, 1.
(7) Liu, N.; Liu, H.; Zhu, S. N.; Giessen, H. *Nat. Photonics* **2009**, *3*, 157.
(8) Hentschel, M.; Schaferling, M.; Weiss, T.; Liu, N.; Giessen, H. *Nano Lett.* **2012**, *12*, 2542.
(9) Decker, M.; Linden, S.; Wegener, M. *Opt. Lett.* **2009**, *34*, 1579.
(10) Guerrero-Martinez, A.; Auguie, B.; Alonso-Gomez, J. L.; Dzolic, Z.; Gomez-Grana, S.; Zinic, M.; Cid, M. M.; Liz-Marzan, L. M. *Angew. Chem., Int. Ed.* **2011**, *50*, 5499.
(11) Kuzyk, A.; Schreiber, R.; Fan, Z. Y.; Pardatscher, G.; Roller, E. M.; Hogele, A.; Simmel, F. C.; Govorov, A. O.; Liedl, T. *Nature* **2012**, *483*, 311.
(12) Chen, C. L.; Zhang, P.; Rosi, N. L. *J. Am. Chem. Soc.* **2008**, *130*, 13555.
(13) Sharma, J.; Chhabra, R.; Cheng, A.; Brownell, J.; Liu, Y.; Yan, H. *Science* **2009**, *323*, 112.
(14) Shen, X.; Song, C.; Wang, J.; Shi, D.; Wang, Z.; Liu, N.; Ding, B. *J. Am. Chem. Soc.* **2012**, *134*, 146.
(15) Mastroianni, A. J.; Claridge, S. A.; Alivisatos, A. P. *J. Am. Chem. Soc.* **2009**, *131*, 8455.
(16) Seeman, N. C. *Nature* **2003**, *421*, 427.
(17) Seeman, N. C. *Nano Lett.* **2010**, *10*, 1971.
(18) Pinheiro, A. V.; Han, D.; Shih, W. M.; Yan, H. *Nat. Nanotechnol.* **2011**, *6*, 763.
(19) Ke, Y.; Ong, L. L.; Shih, W. M.; Yin, P. *Science* **2012**, *338*, 1177.
(20) Smith, D.; Schuller, V.; Engst, C.; Radler, J.; Liedl, T. *Nanomedicine* **2013**, *8*, 105.
(21) Fan, Z.; Govorov, A. O. *Nano Lett.* **2010**, *10*, 2580.
(22) Govorov, A. O.; Fan, Z.; Hernandez, P.; Slocik, J. M.; Naik, R. R. *Nano Lett.* **2010**, *10*, 1374.
(23) Guerrero-Martinez, A.; Alonso-Gomez, J. L.; Auguie, B.; Cid, M. M.; Liz-Marzan, L. M. *Nano Today* **2011**, *6*, 381.
(24) Govorov, A. O.; Gun'ko, Y. K.; Slocik, J. M.; Gerard, V. A.; Fan, Z. Y.; Naik, R. R. *J. Mater. Chem.* **2011**, *21*, 16806.
(25) Fan, Z. Y.; Govorov, A. O. *J. Phys. Chem. C* **2011**, *115*, 13254.
(26) Fan, Z.; Govorov, A. O. *Nano Lett.* **2012**, *12*, 3283.
(27) Rothemund, P. W. *Nature* **2006**, *440*, 297.
(28) Douglas, S. M.; Dietz, H.; Liedl, T.; Hogberg, B.; Graf, F.; Shih, W. M. *Nature* **2009**, *459*, 414.
(29) Dietz, H.; Douglas, S. M.; Shih, W. M. *Science* **2009**, *325*, 725.
(30) Han, D.; Pal, S.; Nangreave, J.; Deng, Z.; Liu, Y.; Yan, H. *Science* **2011**, *332*, 342.
(31) Torring, T.; Voigt, N. V.; Nangreave, J.; Yan, H.; Gothelf, K. V. *Chem. Soc. Rev.* **2011**, *40*, 5636.

(32) García de Abajo, F. J. *Phys. Rev. Lett.* **1999**, *82*, 2776.
(33) García de Abajo, F. J. *Phys. Rev. B* **1999**, *60*, 6086.

dx.doi.org/10.1021/nl400538y | *Nano Lett.* 2013, 13, 2128−2133

3D Plasmonic Chiral Tetramers Assembled by DNA Origami

Xibo Shen,[†] Ana Asenjo-Garcia,[‡] Qing Liu,[†] Qiao Jiang,[†] F. Javier García de Abajo,[‡] Na Liu,[*, §] and Baoquan Ding[*, †]

[†]National Center for Nanoscience and Technology, No. 11 BeiYiTiao, ZhongGuanCun, Beijing 100190, China

[‡]IQFR-CSIC, Serrano 119, 28006 Madrid, Spain

[§]Max-Planck-Institute for Intelligent Systems, Heisenbergstr. 3, D-70569 Stuttgart, Germany

*Address correspondence to dingbq@nanoctr.cn and laura.liu@is.mpg.de

Supporting Information

Experimental Section

Methods:

Preparation of the rectangular DNA origami template. The rectangular DNA origami template was prepared following a standard recipe[1] with several important changes. All the side staples were left out in order to prevent aggregation via helix stacking interactions between adjacent origami. Four groups of capture strands were carefully designed to form four binding sites on the origami template. These capture strands were extended by 18 bases with specific sequences. The mixture was annealed in a ratio of 1:5:10 for M13, capture strands, and staple strands, respectively. It was subsequently assembled in a 1×TAE/Mg^{2+} buffer (Tris, 40 mM; Acetic acid, 20 mM; EDTA, 2 mM; and Magnesium acetate, 12.5 mM; pH 8.0) by slowly cooling it from 90 °C to room temperature. The product was then filtered with a filter device [100 kD, molecular weight cutoff (MWCO), Amicon, Millipore] to remove the extra DNA staple strands and capture strands.

Synthesis of the AuNPs. AuNPs (20 nm) were synthesized by a two-step method.[2] A 1.25 mL $HAuCl_4$ solution (0.2%, w/v) was diluted in 25 mL double-distilled water and heated to boiling. A 1 mL sodium citric solution (1%, w/v; containing 0.05% critic acid) was added to the flask under vigorous stirring. The solution in the flask was kept boiling for 5 minutes under stirring and then cooled at room temperature. 15 nm AuNPs synthesized in this step were used as seeds in the second step. A 6 mL seed solution was diluted in 25 mL double-distilled water. Then a 10 mL $HAuCl_4$ solution (0.02 %, w/v) and a 10 mL ascorbic acid solution (0.02 %, w/v) were added to the seed solution very slowly through a wiggle pump under stirring. Subsequently, the solution was heated to boiling and kept boiling for 20 minutes. The final solution was cooled at room temperature.

Surface modification of the AuNPs with BSPP. BSPP (15 mg) was added to the Au colloidal solution (50 mL) and the mixture was shaken overnight at room temperature. Sodium Chloride (solid) was added slowly to this mixture solution while stirring until the solution color was changed from deep burgundy to light purple. The resulting mixture was centrifuged at 3000 rpm for 30 min and the supernatant was carefully removed with a pipette.

AuNPs were then resuspended in a 1 mL BSPP solution (2.5 mM). Upon mixing with 1mL methanol, the mixture was centrifuged. The supernatant was removed and the AuNPs were resuspended again in a 1 mL BSPP solution (2.5 mM). The concentration of the AuNPs was estimated according to the optical absorption at ~ 519 nm. Phosphine coating increases the amount of negative charges on the AuNP surface and therefore stabilizes the AuNPs at high electrolyte concentrations.

Preparation of AuNP-DNA conjugates. AuNP-DNA conjugates were prepared following a regular protocol.[3] The disulfide bond in the thiol-modified oligonucleotides was reduced to monothiol using TCEP (20 mM, 1 hour) in water. The oligonucleotides were purified using size exclusion columns (G-25, GE Healthcare) to remove small molecules. Monothiol modified oligonucleotides and BSPP modified AuNPs were then incubated in a DNA to Au molar ratio of more than 300:1 in a 0.5 × TBE buffer solution (89 mM Tris, 89 mM boric acid, 2 mM EDTA, pH 8.0, containing 50 mM NaCl) for 20 hours at room temperature. The concentration of NaCl was slowly increased to 300 mM in the subsequent 20 hours in order to increase the binding density of thiolated DNA on AuNPs. AuNP-DNA conjugates were then washed using a 0.5×TBE buffer solution in 100 kDa (MWCO) centrifuge filters to remove the extra free oligonucleotides. The concentration of the AuNP-DNA conjugates was estimated according to the optical absorption at ~ 520 nm. Freshly prepared, fully coated AuNPs do not precipitate in a 1×TAE/$Mg2^{+}$ buffer, preferable for the formation of DNA origami.

Self-assembly of the AuNPs on DNA origami. Purified rectangular DNA origami was mixed with four different AuNP-DNA conjugates in a 1:12 ratio and then annealed from 43 °C to 23 °C for 24 hours.

Purification of the origami-AuNP complexes. The annealed product of the DNA origami and AuNPs was analyzed by agarose gel electrophoresis. The conditions of electrophoresis were as follows: 0.8% Ethidium Bromide stained agarose gel; running buffer, 0.5×TBE buffer; voltage, 15 V/cm; running time, 20 minutes. Selected bands were cut out and the DNA origami-AuNP complexes were extracted from the gel in Freeze-Squeeze columns (Bio-Rad) at 4 °C.

TEM characterization of origami-AuNP complexes. The samples for TEM imaging were prepared by placing a 5 μL of the sample solution on a carbon-coated grid (400 meshes, Ted Pella). Before depositing the sample solution, the grids were treated by negative glow discharge in an Emitch K100X machine. After 10 min deposition, the excess solution was wicked from the grid using filter paper. To remove the deposited salt, the grid was washed with a droplet of water and then the excess water was wicked away using filter paper. The grid was kept at room temperature for 3 hours for drying. The TEM characterization was conducted using a Tecnei G2-20S TWIN system, operated at 200 kV with a bright field mode.

Optical characterization. The CD spectra were measured by a Jasco J-810 spectropolarimeter. The Ultraviolet-visible absorption spectra were recorded using a UV-VIS spectrophotometer (UV-2450, Shimadzu).

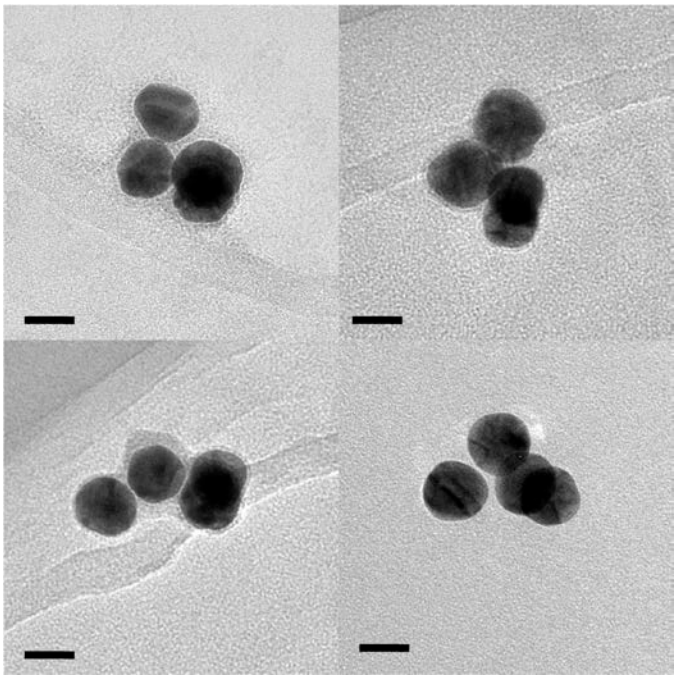

Figure S1. Additional TEM images of the right-handed plasmonic tetramers (scale bar: 20 nm).

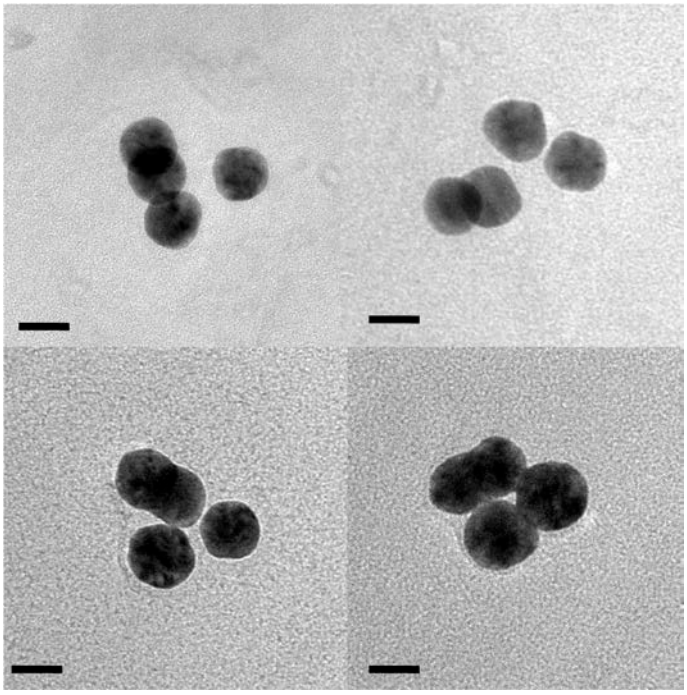

Figure S2. Additional TEM images of the left-handed plasmonic tetramers (scale bar: 20 nm).

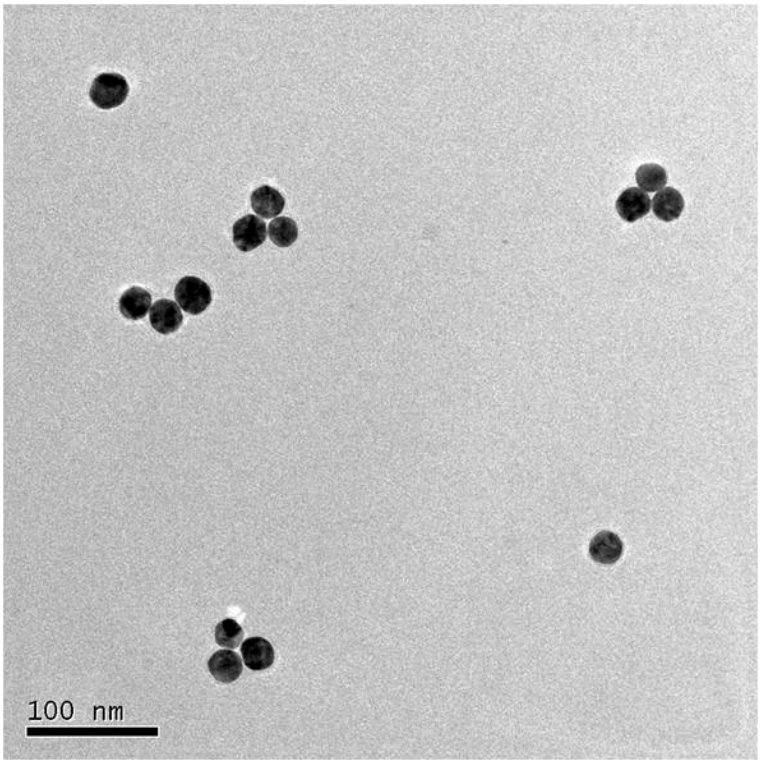

Figure S3. TEM images of the achiral plasmonic nanostructures. Three AuNPs are assembled on the same surface side of the DNA origami.

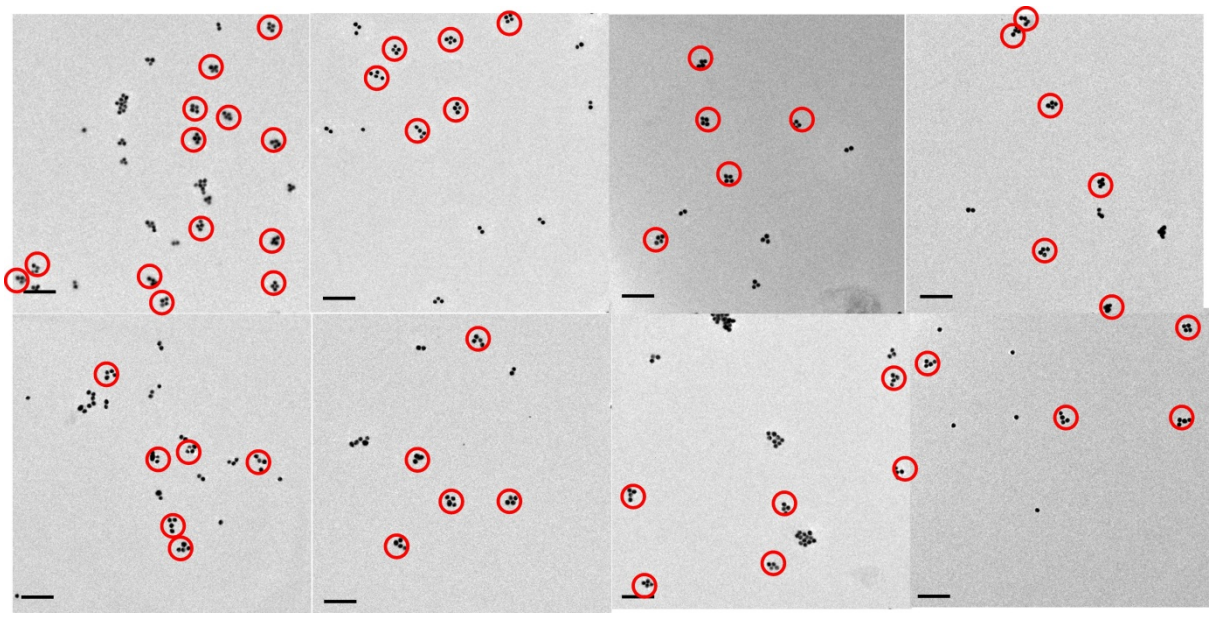

Figure S4. Additional TEM images of the left-handed plasmonic tetramers (scale bar: 200nm).

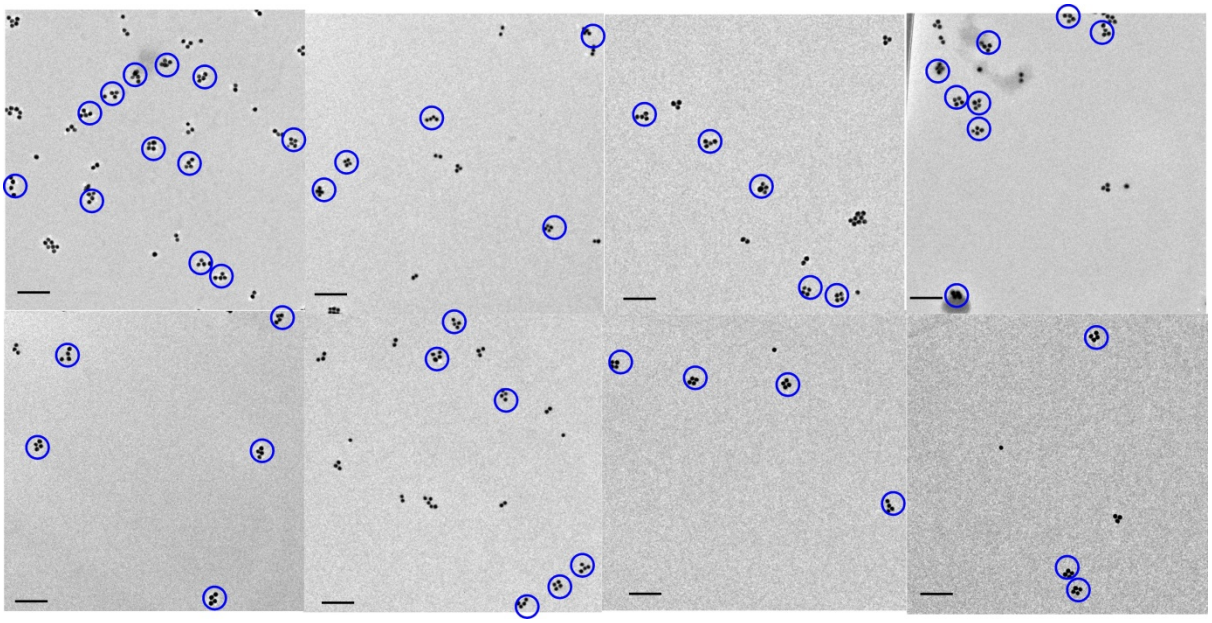

Figure S5. Additional TEM images of the right-handed plasmonic tetramers (scale bar: 200nm).

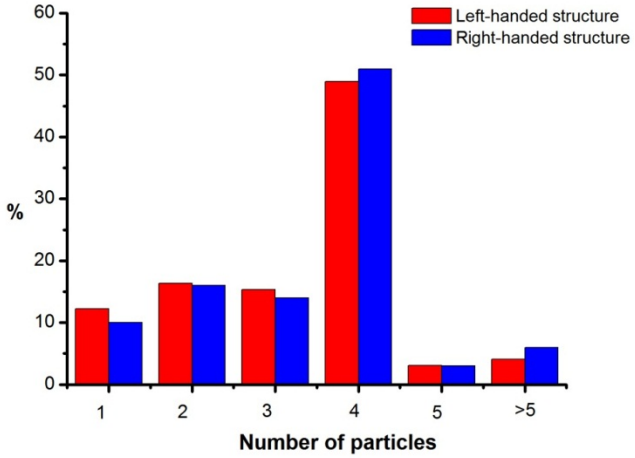

Figure S6. Statistic chart of the numbers of AuNPs assembled on the left and right-handed plasmonic tetramers.

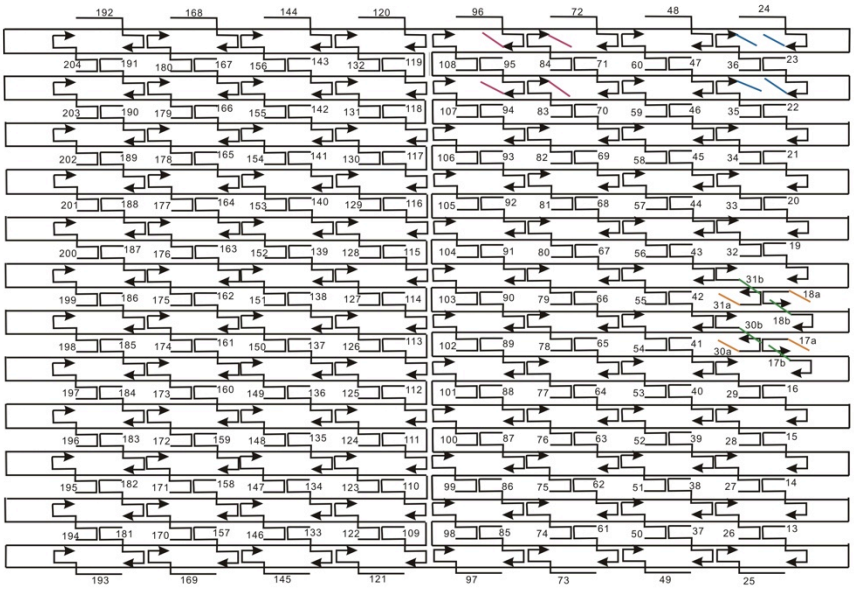

Figure S7. Schematic diagram of the binding sites for the right-handed structure. The lines in four different colors represent the four different types of the extended capture strands with specific sequences.

Capture strands for the right-handed structure

There were a total of 16 staple strands modified with sticky ends to organize four AuNPs. The sequence of the staple strands (left to right: 5'-3') is as follows:

23, GAGAATAGCTTTTGCGGGATCGTCGGGTAGCATTCGCATTCAGGATTCTC
24, ACGTTAGTAAATGAATTTTCTGTAAGCGGAGTTTCGCATTCAGGATTCTC
35, GCTCCATGAGAGGCTTTGAGGACTAGGGAGTTTTCGCATTCAGGATTCTC
36, AAAGGCCGAAAGGAACAACTAAAGCTTTCCAGTTCGCATTCAGGATTCTC
17a, AAAAAAAAAAAAAAAAATTCTGTAATATTGCCTGA
18a, AAAAAAAAAAAAAAAAATTTGCAACTAAGCAATAA
30a, AAAAAAAAAAAAAAAAATTTCAGGTCACTTTTGCG
31a, AAAAAAAAAAAAAAAAATTCAAAATTAAAGTACGG
17b, ATTATTATTATTATTATTTTGAGTCTGGAAAACTAG
18b, ATTATTATTATTATTATTTTAGCCTCAGTTATGACC
30b, ATTATTATTATTATTATTTTGGAGAAGCAGAATTAG
31b, ATTATTATTATTATTATTTTTGTCTGGAAGAGGTCA
83, GCGAAACATGCCACTACGAAGGCATGCGCCGATTAGACTCTAATGCAGTC
84, CAATGACACTCCAAAAGGAGCCTTACAACGCCTTAGACTCTAATGCAGTC
95, TCGGTTTAGCTTGATACCGATAGTCCAACCTATTAGACTCTAATGCAGTC
96, TGAGTTTCGTCACCAGTACAAACTTAATTGTATTAGACTCTAATGCAGTC

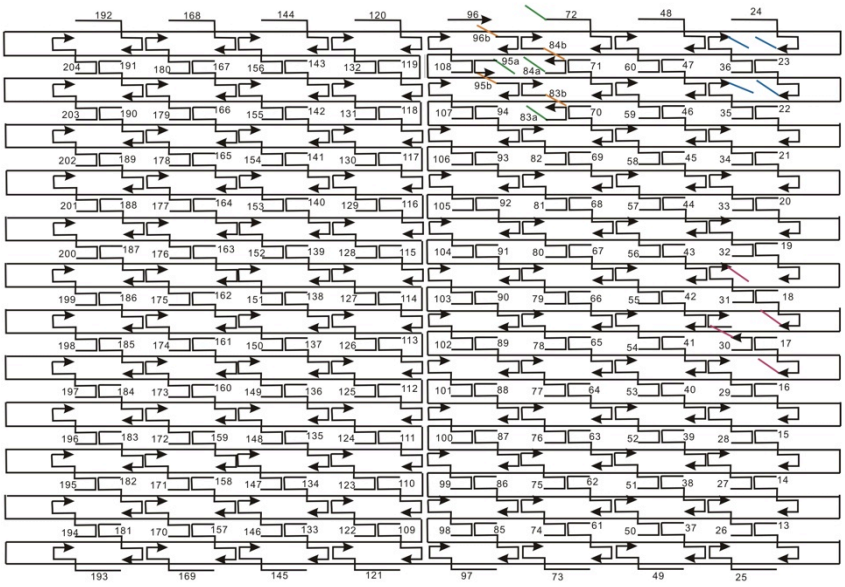

Figure S8. Schematic diagram of the binding sites for the left-handed structure. The lines in four different colors represent the four different types of the extended capture strands with specific sequences.

Capture strands for the left-handed structure

There were a total of 16 staple strands modified with sticky ends to organize four AuNPs. The sequence of the staple strands (left to right: 5'-3') is as follows:

23, GAGAATAGCTTTTGCGGGATCGTCGGGTAGCATTCGCATTCAGGATTCTC
24, ACGTTAGTAAATGAATTTTCTGTAAGCGGAGTTTCGCATTCAGGATTCTC
35, GCTCCATGAGAGGCTTTGAGGACTAGGGAGTTTTCGCATTCAGGATTCTC
36, AAAGGCCGAAAGGAACAACTAAAGCTTTCCAGTTCGCATTCAGGATTCTC
17, CTGTAATATTGCCTGAGAGTCTGGAAAACTAGTTAGACTCTAATGCAGTC
18, TGCAACTAAGCAATAAAGCCTCAGTTATGACCTTAGACTCTAATGCAGTC
30, TCAGGTCACTTTTGCGGGAGAAGCAGAATTAGTTAGACTCTAATGCAGTC
31, CAAAATTAAAGTACGGGTCTGGAAGAGGTCATTAGACTCTAATGCAGTC
83a, ATTATTATTATTATTATTTTGCGAAACATGCCACTA
84a, ATTATTATTATTATTATTTTGGAGCCTTACAACGCC
95a, ATTATTATTATTATTATTTTCCGATAGTCCAACCTA
96a, ATTATTATTATTATTATTTTTACAAACTTAATTGTA
83b, AAAAAAAAAAAAAAAATTCGAAGGCATGCGCCGA
84b, AAAAAAAAAAAAAAAATTCAATGACACTCCAAAA
95b, AAAAAAAAAAAAAAAATTTCGGTTTAGCTTGATA
96b, AAAAAAAAAAAAAAAATTTGAGTTTCGTCACCAG

Thiolated strands that covered the AuNPs

S25A, HS-TTTTGAGA ATCCTG AATGCG
S25B, HS-TTTTGACTGCATTAGAGTCT

S25C, ATTATT ATTATT ATT TTTT-SH
S25D, TTTTTT TTTTTT TTT TTTT-SH

Sequences used in the assembly of the DNA origami template

13 TGGTTTTTAACGTCAAAGGGCGAAGAACCATC
14 CTTGCATGCATTAATGAATCGGCCCGCCAGGG
15 TAGATGGGGGGTAACGCCAGGGTTGTGCCAAG
16 CATGTCAAGATTCTCCGTGGGAACCGTTGGTG
17 CTGTAATATTGCCTGAGAGTCTGGAAAACTAG
18 TGCAACTAAGCAATAAAGCCTCAGTTATGACC
19 AAACAGTTGATGGCTTAGAGCTTATTTAAATA
20 ACGAACTAGCGTCCAATACTGCGGAATGCTTT
21 CTTTGAAAAGAACTGGCTCATTATTTAATAAA
22 ACGGCTACTTACTTAGCCGGAACGCTGACCAA
23 GAGAATAGCTTTTGCGGGATCGTCGGGTAGCA
24 ACGTTAGTAAATGAATTTTCTGTAAGCGGAGT
25 ACCCAAATCAAGTTTTTTGGGGTCAAAGAACG
26 TGGACTCCCTTTTCACCAGTGAGACCTGTCGT
27 GCCAGCTGCCTGCAGGTCGACTCTGCAAGGCG
28 ATTAAGTTCGCATCGTAACCGTGCGAGTAACA
29 ACCCGTCGTCATATGTACCCCGGTAAAGGCTA
30 TCAGGTCACTTTTGCGGGAGAAGCAGAATTAG
31 CAAAATTAAAGTACGGTGTCTGGAAGAGGTCA
32 TTTTTGCGCAGAAAACGAGAATGAATGTTTAG
33 ACTGGATAACGGAACAACATTATTACCTTATG
34 CGATTTTAGAGGACAG ATGAACGGCGCGACCT
35 GCTCCATGAGAGGCTT TGAGGACTAGGGAGTT
36 AAAGGCCGAAAGGAACAACTAAAGCTTTCCAG
37 AGCTGATTACAAGAGTCCACTATTGAGGTGCC
38 CCCGGGTACTTTCCAGTCGGGAAACGGGCAAC
39 GTTTGAGGGAAAGGGGGATGTGCTAGAGGATC
40 AGAAAAGCAACATTAAATGTGAGCATCTGCCA
41 CAACGCAATTTTTGAGAGATCTACTGATAATC
42 TCCATATACATACAGGCAAGGCAACTTTATTT
43 CAAAAATCATTGCTCCTTTTGATAAGTTTCAT
44 AAAGATTCAGGGGGTAATAGTAAACCATAAAT
45 CCAGGCGCTTAATCATTGTGAATTACAGGTAG
46 TTTCATGAAAATTGTGTCGAAATCTGTACAGA
47 AATAATAAGGTCGCTGAGGCTTGCAAAGACTT
48 CGTAACGATCTAAAGTTTTGTCGTGAATTGCG
49 GTAAAGCACTAAATCGGAACCCTAGTTGTTCC
50 AGTTTGGAGCCCTTCACCGCCTGGTTGCGCTC

51 ACTGCCCGCCGAGCTCGAATTCGTTATTACGC
52 CAGCTGGCGGACGACGACAGTATCGTAGCCAG
53 CTTTCATCCCCAAAAACAGGAAGACCGGAGAG
54 GGTAGCTAGGATAAAAATTTTTAGTTAACATC
55 CAATAAATACAGTTGATTCCCAATTTAGAGAG
56 TACCTTTAAGGTCTTTACCCTGACAAAGAAGT
57 TTTGCCAGATCAGTTGAGATTTAGTGGTTTAA
58 TTTCAACTATAGGCTGGCTGACCTTGTATCAT
59 CGCCTGATGGAAGTTTCCATTAAACATAACCG
60 ATATATTCTTTTTTCACGTTGAAAATAGTTAG
61 GAGTTGCACGAGATAGGGTTGAGTAAGGGAGC
62 TCATAGCTACTCACATTAATTGCGCCCTGAGA
63 GAAGATCGGTGCGGGCCTCTTCGCAATCATGG
64 GCAAATATCGCGTCTGGCCTTCCTGGCCTCAG
65 TATATTTTAGCTGATAAATTAATGTTGTATAA
66 CGAGTAGAACTAATAGTAGTAGCAAACCCTCA
67 TCAGAAGCCTCCAACAGGTCAGGATCTGCGAA
68 CATTCAACGCGAGAGGCTTTTGCATATTATAG
69 AGTAATCTTAAATTGGGCTTGAGAGAATACCA
70 ATACGTAAAAGTACAACGGAGATTTCATCAAG
71 AAAAAAGGACAACCATCGCCCACGCGGGTAAA
72 TGTAGCATTCCACAGACAGCCCTCATCTCCAA
73 CCCCGATTTAGAGCTTGACGGGGAAATCAAAA
74 GAATAGCCGCAAGCGGTCCACGCTCCTAATGA
75 GTGAGCTAGTTTCCTGTGTGAAATTTGGGAAG
76 GGCGATCGCACTCCAGCCAGCTTTGCCATCAA
77 AAATAATTTTAAATTGTAAACGTTGATATTCA
78 ACCGTTCTAAATGCAATGCCTGAGAGGTGGCA
79 TCAATTCTTTTAGTTTGACCATTACCAGACCG
80 GAAGCAAAAAAGCGGATTGCATCAGATAAAAA
81 CCAAAATATAATGCAGATACATAAACACCAGA
82 ACGAGTAGTGACAAGAACCGGATATACCAAGC
83 GCGAAACATGCCACTACGAAGGCATGCGCCGA
84 CAATGACACTCCAAAAGGAGCCTTACAACGCC
85 CCAGCAGGGGCAAAATCCCTTATAAAGCCGGC
86 GCTCACAATGTAAAGCCTGGGGTGGGTTTGCC
87 GCTTCTGGTCAGGCTGCGCAACTGTGTTATCC
88 GTTAAAATTTTAACCAATAGGAACCCGGCACC
89 AGGTAAAGAAATCACCATCAATATAATATTTT
90 TCGCAAATGGGGCGCGAGCTGAAATAATGTGT
91 AAGAGGAACGAGCTTCAAAGCGAAGATACATT
92 GGAATTACTCGTTTACCAGACGACAAAAGATT
93 CCAAATCACTTGCCCTGACGAGAACGCCAAAA
94 AAACGAAATGACCCCCAGCGATTATTCATTAC

95 TCGGTTTAGCTTGATACCGATAGTCCAACCTA
96 TGAGTTTCGTCACCAGTACAAACTTAATTGTA
97 GAACGTGGCGAGAAAGGAAGGGAACAAACTAT
98 CCGAAATCCGAAAATCCTGTTTGAAGCCGGAA
99 GCATAAAGTTCCACACAACATACGAAGCGCCA
100 TTCGCCATTGCCGGAAACCAGGCATTAAATCA
101 GCTCATTTTCGCATTAAATTTTTGAGCTTAGA
102 AGACAGTCATTCAAAAGGGTGAGAAGCTATAT
103 TTTCATTTGGTCAATAACCTGTTTATATCGCG
104 TTTTAATTGCCCGAAAGACTTCAAAACACTAT
105 CATAACCCGAGGCATAGTAAGAGCTTTTTAAG
106 GAATAAGGACGTAACAAAGCTGCTCTAAAACA
107 CTCATCTTGAGGCAAAAGAATACAGTGAATTT
108 CTTAAACATCAGCTTGCTTTCGAGCGTAACAC
109 ACGAACCAAAACATCGCCATTAAATGGTGGTT
110 CGACAACTAAGTATTAGACTTTACAATACCGA
111 CTTTTACACAGATGAATATACAGTAAACAATT
112 TTAAGACGTTGAAAACATAGCGATAACAGTAC
113 GCGTTATAGAAAAAGCCTGTTTAGAAGGCCGG
114 ATCGGCTGCGAGCATGTAGAAACCTATCATAT
115 CCTAATTTACGCTAACGAGCGTCTAATCAATA
116 AAAAGTAATATCTTACCGAAGCCCTTCCAGAG
117 TTATTCATAGGGAAGGTAAATATTCATTCAGT
118 GAGCCGCCCCACCACCGGAACCGCGACGGAAA
119 AATGCCCCGTAACAGTGCCCGTATCTCCCTCA
120 CAAGCCCAATAGGAACCCATGTACAAACAGTT
121 CGGCCTTGCTGGTAATATCCAGAACGAACTGA
122 TAGCCCTACCAGCAGAAGATAAAAACATTTGA
123 GGATTTAGCGTATTAAATCCTTTGTTTTCAGG
124 TTTAACGTTCGGGAGAAACAATAATTTTCCCT
125 TAGAATCCCTGAGAAGAGTCAATAGGAATCAT
126 AATTACTACAAATTCTTACCAGTAATCCCATC
127 CTAATTTATCTTTCCTTATCATTCATCCTGAA
128 TCTTACCAGCCAGTTACAAAATAAATGAAATA
129 GCAATAGCGCAGATAGCCGAACAATTCAACCG
130 ATTGAGGGTAAAGGTGAATTATCAATCACCGG
131 AACCAGAGACCCTCAGAACCGCCAGGGGTCAG
132 TGCCTTGACTGCCTATTTCGGAACAGGGATAG
133 AGGCGGTCATTAGTCTTTAATGCGCAATATTA
134 TTATTAATGCCGTCAATAGATAATCAGAGGTG
135 CCTGATTGAAAGAAATTGCGTAGACCCGAACG
136 ATCAAAATCGTCGCTATTAATTAACGGATTCG
137 ACGCTCAAAATAAGAATAAACACCGTGAATTT
138 GGTATTAAGAACAAGAAAAATAATTAAAGCCA

139 ATTATTTAACCCAGCTACAATTTTCAAGAACG
140 GAAGGAAAATAAGAGCAAGAAACAACAGCCAT
141 GACTTGAGAGACAAAAGGGCGACAAGTTACCA
142 GCCACCACTCTTTTCATAATCAAACCGTCACC
143 CTGAAACAGGTAATAAGTTTTAACCCCTCAGA
144 CTCAGAGCCACCACCCTCATTTTCCTATTATT
145 CCGCCAGCCATTGCAACAGGAAAAATATTTTT
146 GAATGGCTAGTATTAACACCGCCTCAACTAAT
147 AGATTAGATTTAAAAGTTTGAGTACACGTAAA
148 ACAGAAATCTTTGAATACCAAGTTCCTTGCTT
149 CTGTAAATCATAGGTCTGAGAGACGATAAATA
150 AGGCGTTACAGTAGGGCTTAATTGACAATAGA
151 TAAGTCCTACCAAGTACCGCACTCTTAGTTGC
152 TATTTTGCTCCCAATCCAAATAAGTGAGTTAA
153 GCCCAATACCGAGGAAACGCAATAGGTTTACC
154 AGCGCCAACCATTTGGGAATTAGATTATTAGC
155 GTTTGCCACCTCAGAGCCGCCACCGATACAGG
156 AGTGTACTTGAAAGTATTAAGAGGCCGCCACC
157 GCCACGCTATACGTGGCACAGACAACGCTCAT
158 ATTTTGCGTCTTTAGGAGCACTAAGCAACAGT
159 GCGCAGAGATATCAAAATTATTTGACATTATC
160 TAACCTCCATATGTGAGTGAATAAACAAAATC
161 CATATTTAGAAATACCGACCGTGTTACCTTTT
162 CAAGCAAGACGCGCCTGTTTATCAAGAATCGC
163 TTTTGTTTAAGCCTTAAATCAAGAATCGAGAA
164 ATACCCAAGATAACCCACAAGAATAAACGATT
165 AATCACCAAATAGAAAATTCATATATAACGGA
166 CACCAGAGTTCGGTCATAGCCCCCGCCAGCAA
167 CCTCAAGAATACATGGCTTTTGATAGAACCAC
168 CCCTCAGAACCGCCACCCTCAGAACTGAGACT
169 GGAAATACCTACATTTTGACGCTCACCTGAAA
170 GCGTAAGAGAGAGCCAGCAGCAAAAAGGTTAT
171 CTAAAATAGAACAAAGAAACCACCAGGGTTAG
172 AACCTACCGCGAATTATTCATTTCCAGTACAT
173 AAATCAATGGCTTAGGTTGGGTTACTAAATTT
174 AATGGTTTACAACGCCAACATGTAGTTCAGCT
175 AATGCAGACCGTTTTTATTTTCATCTTGCGGG
176 AGGTTTTGAACGTCAAAAATGAAAGCGCTAAT
177 ATCAGAGAAAGAACTGGCATGATTTTATTTTG
178 TCACAATCGTAGCACCATTACCATCGTTTTCA
179 TCGGCATTCCGCCGCCAGCATTGACGTTCCAG
180 TAAGCGTCGAAGGATTAGGATTAGTACCGCCA
181 CTAAAGCAAGATAGAACCCTTCTGAATCGTCT
182 CGGAATTATTGAAAGGAATTGAGGTGAAAAAT

183 GAGCAAAAACTTCTGAATAATGGAAGAAGGAG
184 TATGTAAACCTTTTTTAATGGAAAAATTACCT
185 AGAGGCATAATTTCATCTTCTGACTATAACTA
186 TCATTACCCGACAATAAACAACATATTTAGGC
187 CTTTACAGTTAGCGAACCTCCCGACGTAGGAA
188 TTATTACGGTCAGAGGGTAATTGAATAGCAGC
189 CCGGAAACACACCACGGAATAAGTAAGACTCC
190 TGAGGCAGGCGTCAGACTGTAGCGTAGCAAGG
191 TGCTCAGTCAGTCTCTGAATTTACCAGGAGGT
192 TATCACCGTACTCAGGAGGTTTAGCGGGGTTT
193 GAAATGGATTATTTACATTGGCAGACATTCTG
194 GCCAACAGTCACCTTGCTGAACCTGTTGGCAA
195 ATCAACAGTCATCATATTCCTGATTGATTGTT
196 TGGATTATGAAGATGATGAAACAAAATTTCAT
197 TTGAATTATGCTGATGCAAATCCACAAATATA
198 TTTTAGTTTTTCGAGCCAGTAATAAATTCTGT
199 CCAGACGAGCGCCCAATAGCAAGCAAGAACGC
200 GAGGCGTTAGAGAATAACATAAAAGAACACCC
201 TGAACAAACAGTATGTTAGCAAACTAAAAGAA
202 ACGCAAAGGTCACCAATGAAACCAATCAAGTT
203 TGCCTTTAGTCAGACGATTGGCCTGCCAGAAT
204 GGAAAGCGACCAGGCGGATAAGTGAATAGGTG

The sequence of the single stranded circular M13mp18 viral DNA (purchased from New England Biolabs) can be found at:
http://www.neb.com/nebecomm/tech_reference/restriction_enzyme/sequences/13mp18.txt

Theoretical Section

Theory and modeling

Chirality is present in many biologically active molecules, such as amino acids and sugars. It can also occur in artificial structures with chiral arrangements of non-chiral objects. Specifically, four AuNPs assembled by DNA origami can lead to the formation of plasmonic chiral tetramers. Basically, four is the minimum number of particles that allows for obtaining 3D chirality, as beautifully explained from a simple particles-as-dipoles picture [4].

In our calculation, rather than relying on just dipoles, we use a full multipolar expansion of the electromagnetic field around each AuNP in the tetramer. The self-consistent interaction among these multipoles allows us to calculate the extinction cross-sections for left and right circularly polarized light, respectively, from which we obtain the CD spectra. A multiple elastic scattering of multipolar expansions code (MESME) is used for this purpose [5, 6].

The orientations of the chiral assemblies in the solution are totally random, and

accordingly, we carry out an average over the angles of the incident light (or equivalently, over all possible assembly orientations for fixed light incidence). The CD signal can then be expressed as

$$CD \propto \langle \sigma_L - \sigma_R \rangle_\Omega \tag{1}$$

where σ_L and σ_R are the extinction cross-sections for the left and right circularly polarized light, respectively, and $< >_\Omega$ denotes the average over the solid angle of the tetramer orientations. This average is approximated by

$$\langle \sigma_{L,R} \rangle_\Omega \simeq \frac{1}{4\pi} \frac{2\pi^2}{N_\theta N_\varphi} \sum_{i,j} \sigma_{L,R}(\theta_i, \varphi_j) \sin\theta_i \tag{2}$$

where the polar and azimuthal angles are in the ranges of $\theta_i \in [0,\pi)$ in N_θ=50 steps and $\varphi_i \in [0,2\pi)$ in N_φ=100 steps, respectively, covering 5,000 orientations.

From this expression, we can obtain the ellipticity (in mdeg) [4] (this is actually the quantity measured in the experiment) by taking into account the chiral assembly concentration (c = 0.3 nM) and the optical path length (l = 0.5 cm):

$$\theta(\text{mdeg}) = \frac{45 N_A}{\pi} \langle \sigma_L - \sigma_R \rangle_\Omega \, (\text{cm}^2) \cdot c(\text{M}) \cdot l(\text{cm}) \tag{3}$$

The dielectric function of gold is taken from tabulated optical data [7]. The chiral assembly is in water (refractive index 1.33). We ignore the presence of the DNA in our simulations. This is a safe assumption because the DNA occupies a small volume in our case and its dielectric constant is non-resonant and has small contrast with water. DNA is a chiral molecule and exhibits circular dichroism in the ultraviolet range, where DNA strongly absorbs light [8]. Although it has been demonstrated that natural chiral molecules attached to nonchiral plasmonic particles may induce CD at optical wavelengths [9-11], the circular dichroism reported here is mostly related to the chiral arrangement of the AuNPs and their strong plasmonic resonant coupling, as demonstrated in the control experiment showed in Fig. 3b of the main paper (black curve).

Although the exact diameter and separation of the AuNPs are not known, it is possible to estimate their average values by comparing the calculated results to the extinction cross-section spectra of the chiral assemblies and the dip-peak positions in the CD spectra obtained from the experiment. The experimental results are consistent with the calculated results when 20 nm AuNPs and a 8 nm inter-particle separation are utilized. Larger particles lead to a spectral redshift relative to the experimental data in both the extinction cross-section and the CD spectra.

The difference between the extinction cross-sections of the left and right circularly polarized light is actually very small. The difference at the CD maximum is

$$\frac{\langle \sigma_L - \sigma_R \rangle_\Omega}{\langle \sigma_L + \sigma_R \rangle_\Omega} \simeq 0.1\% \tag{4}$$

However, such a small difference produces experimentally resolvable CD. As shown in Fig. 3b of the main paper, theory agrees qualitatively well with experiment, although the measured CD amplitudes are smaller than those predicted by theory. The main reason for this discrepancy lies in the assessment of the concentration of the chiral plasmonic tetramers, as we argue in the main paper.

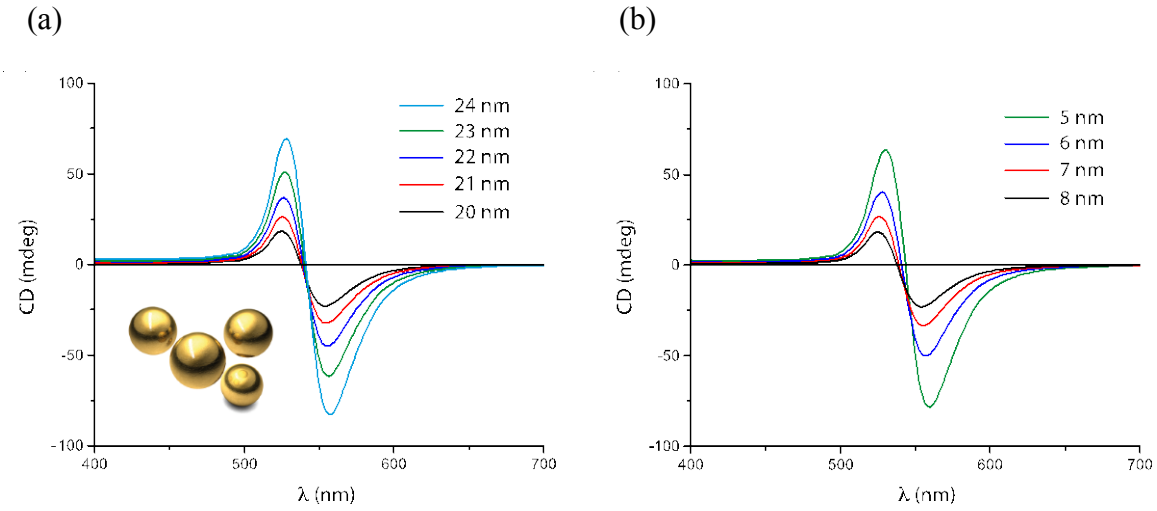

Figure S9. Influence of the size and separation of the AuNPs on the CD spectra. The calculations are carried out based on Eq. (3) for the chiral assembly that is shown in the inset. (a) CD for different AuNP diameters and a fixed AuNP separation of 8 nm. (b) CD for different separation distances and a fixed AuNP diameter of 20 nm.

As shown in Fig. S9, decreasing the particle size and increasing the inter-particle distance can lead to a dramatic reduction of the CD signal because of the weakened interaction among the AuNPs. For a chiral assembly formed by 20 nm AuNPs separated by 8 nm, the rotation of the field vector along the assembly at the wavelength of maximum dichroism is ~30º. When the field propagates along larger assemblies, the degree of rotation increases, and therefore the CD is also more pronounced. Another important factor that contributes to explain the smaller experimental signal with respect to the theoretical prediction is the uncertainty in the relative positions of the AuNPs in the individual chiral assemblies. As shown by Kuzyk *et al*. [12], the CD bisignate pattern is robust against this source of disorder in a helical configuration, but it has a more substantial effect in tetramers with a smaller number of particles (i.e., uncertainties in the position of any of the particles are more relevant to the response of the entire AuNP assembly).

Mode excitation

Under illumination with different light polarizations or incident angles, the plasmonic modes of the chiral assembly display different intensities. This effect is analyzed in Fig. S10. The black curve represents the difference of the extinction cross-sections between the left and right circularly polarized light averaged over all assembly orientations, as discussed above. The blue and red curves correspond to the incidence directions indicated in the inset. Interestingly, it is also possible to obtain an angular averaged curve within <1% error relative

to the black curve by just averaging the six spectra obtained from the six different incidence configurations, which are along three orthogonal directions as shown in the inset [13]. Obviously, the magnitude of the CD signal for specific directions of incidence is larger than the average, and sign changes in the CD signal may occur, depending on the angle-dependent relative excitation amplitudes of the different modes.

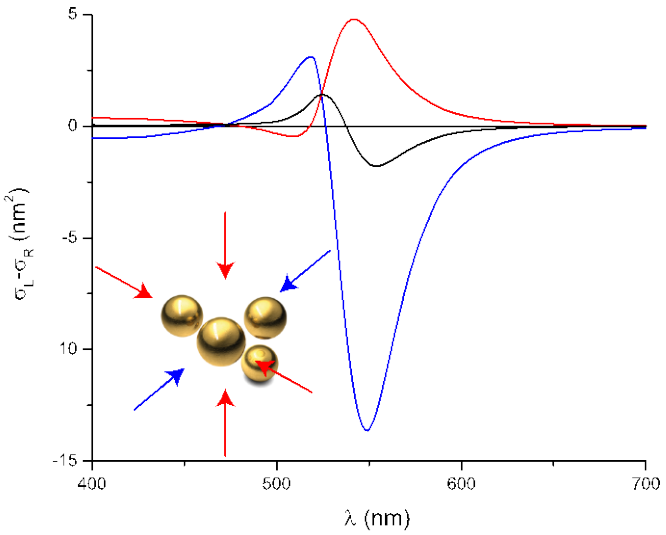

Figure S10. Influence of the incidence direction on the CD. Inset: 20 nm AuNP assembly with a particle spacing of 8 nm. The red and blue curves correspond to the results under the specific light incidence directions shown in the inset. The black curve is the average over the spectra obtained from the six different incidence configurations.

References

[1] K. Lund, A. J. Manzo, N. Dabby, N. Michelotti, A. Johnson-Buck, J. Nangreave, S. Taylor, R. J. Pei, M. N. Stojanovic, N. G. Walter, E. Winfree, H. Yan, Molecular robots guided by prescriptive landscapes, *Nature* **2010**, 465, 206-210.

[2] C. Ziegler, A. Eychmuller, Seeded Growth Synthesis of Uniform Gold Nanoparticles with Diameters of 15-300 nm, *J. Phys. Chem. C* **2011**, *115*, 4502-4506.

[3] B. Q. Ding, Z. T. Deng, H. Yan, S. Cabrini, R. N. Zuckermann, J. Bokor, Gold Nanoparticle Self-Similar Chain Structure Organized by DNA Origami, *J. Am. Chem. Soc.* **2010**, *132*, 3248-3249

[4] Z. Fan, and A. O. Govorov, Plasmonic circular dichroism of metal nanoparticle assemblies, *Nano Lett.* **2010**, 10, 2580–2587.

[5] F. J. García de Abajo, Interaction of radiation and fast electrons with clusters of dielectrics: A multiple scattering approach, *Phys. Rev. Lett.* **1999**, 82, 2776-2779.

[6] F. J. García de Abajo, Multiple scattering of radiation in clusters of dielectrics, *Phys. Rev. B* **1999**, 60, 6086-6102.

[7] P. B. Johnson, and R. W. Christy, Optical constants of the noble metals, *Phys. Rev. B* **1972**, 6, 4370-4379.

[8] Berova, N.; Nakanishi, K.; Woody, R. W.: Circular dichroism : principles and applications. *VCH Pub* 1994.

[9] I. Lieberman, G. Shemer, T. Fried, E. M. Kosower, and G. Markovich, Plasmon-resonance-enhanced absorption and circular dichroism, *Angew. Chem. Int. Ed.* **2008**, 47, 4855–4857.

[10] A. O. Govorov, Z. Fan P. Hernandez, J. M. Slocik, and R. R. Naik, Theory of circular dichroism of nanomaterials comprising chiral molecules and nanocrystals: Plasmon enhancement, dipole interactions, and dielectric effects, *Nano Lett.* **2010***,* 10, 1374–1384.

[11] J. M. Slocik, A. O. Govorov, and R. R. Naik, Plasmonic circular dichroism of peptide- functionalized gold nanoparticles, *Nano Lett.* **2011***,* 11, 701–705.

[12] A. Kuzyk, R. Schreiber, Z. Fan, G. Pardatscher, E. M. Roller, A. Hogele, F. C. Simmel, A. O. Govorov, and T. Liedl, DNA-based self-assembly of chiral plasmonic nano-structures with tailored optical response, *Nature* **2012***,* 483, 311-314.

[13] Z. Fan, and A. O. Govorov, Chiral nanocrystals: plasmonic spectra and circular dichroism, *Nano Lett.* **2012**, 12, 3283-3289.